Robust Receivers for Base Station Cooperation Systems

F. Casal Ribeiro[(1,2)], J. Guerreiro[(1,3)], R. Dinis[(1,3)], F. Cercas[(1,2)], A. Silva[(1,4)]
[(1)] IT - Instituto de Telecomunicações, Portugal
[(2)] ISCTE - Instituto Universitário de Lisboa, Portugal
[(3)] FCT - Universidade Nova de Lisboa, Portugal
[(4)] DETI - Universidade de Aveiro, Portugal

Abstract - In BS (Base Station) cooperation architectures the MTs (Mobile Terminals) in adjacent cells can operate in the same frequency, with the signal's separation and/or MTs detection being performed by a CPU (Central Processing Unit). This results in a substantial improvement in the overall system's capacity and spectral efficiency when compared to conventional cellular systems. To decrease the data load in the backhaul links, the received signals at a given BS must be sampled and quantized before being sent to the CPU, which results in a significant increase of quantization errors. We consider the uplink of BS cooperation schemes employing SC-FDE (Single-Carrier with Frequency-Domain Equalization) modulations and a detection performed through receivers based on the IB-DFE (Iterative Block Decision Feedback Equalization) concept. We present accurate approaches for obtaining the spectral characterization of the quantization noise. Moreover, we propose the design of robust receivers that can take into account the quantization noise effects [1].

Index Terms: BS Cooperation, SC-FDE, IB-DFE, Quantization

I. Introduction

The frequency spectrum is a scarce and expensive resource and its efficient management will be the key factor in the medium and long term future regarding cellular systems, such as 5G networks. In order to avoid inter-cell interference in conventional architectures, MTs (Mobile Terminals) transmit at distinct frequencies in different cells, which can lead to a lower quality of the system's overall performance due to the reuse factors implemented. Therefore, future cellular systems designs must focus on the improvements of interference-mitigation techniques, namely a cooperation scheme of the elements from the network. Following the cooperation concept, BS (Base Station) cooperation systems are a reliable alternative to the current cellular implementations. In this multi-cell cooperation idea, different cells are no longer considered as separate entities with each MT being assigned a specific BS, but instead users in adjacent cells can share the same physical channel (i.e., they transmit at the same frequency) and the signals between different MTs and BSs are collected and processed by a CPU (Central Processing Unit), so as to perform the user separation and/or interference mitigation. Hence, with BS cooperation it is possible to have a universal frequency reuse and considerable macro-diversity effects, improving the coverage and power requirements in each individual link. In the downlink transmission of BS cooperation systems, considering that a correct signal separation is provided, this is achieved by the implementation of appropriate pre-processing schemes [2], [3]. This paper focus on the uplink transmission, where the global signal contributions from all MTs received at each BS are sent to a CPU that operates the required signal separation and correctly detects data blocks that are then sent to the corresponding BS [4].

Block transmission techniques, jointly with frequency-domain processing schemes are suitable for broadband wireless systems, where the two main techniques include OFDM (Orthogonal Frequency Division Multiplexing) [5] and SC-FDE (Single-Carrier with Frequency Domain Equalization) [6], [7]. For the uplink it is preferable to use SC-FDE modulations instead of OFDM. Although they have similar overall signal processing requirements and achievable performances, the receiver complexity is higher for SC-FDE and the transmitter complexity is higher for OFDM. Moreover, the envelope fluctuations of

[1]This work was partially published in [1].

OFDM signals are much higher than the envelope of single-carrier signals with the same constellations, indicating that OFDM is clearly preferable for the downlink while SC-FDE is more suitable for the uplink transmission [8], [9].

In this work, the signals from the different MTs received at a given BS are collected, sampled and quantized by an ADC (Analog-to-Digital Converter), with the objective of decrease the overall backhaul communication requirements. Posteriorly, at the CPU, the signal separation methodology is performed through frequency-domain receivers based on the IB-DFE (Iterative Block Decision Feedback Equalization) concept [10], [11]. Regarding the sampled and quantized signals, the resulting quantization noise can lead to substantial performance degradation, so if the spectral characteristics of the quantization noise is known, it is possible to design robust receivers that can cope with the corresponding degradation. The normal approach for obtaining the PSD (Power Spectral Density) of the quantization noise is to consider it with uniform distribution [12]. However, this approach is only accurate for quantizers with high quantization levels but no saturation effects. Since the signals that are received at each BS present Gaussian-like characteristics, it is possible to obtain the quantization noise variance according to [13], as long as the signal to be quantized has a flat spectrum [14]. Gaussian approximation is reasonable for multipath channels, even with a single user. However, this approach is only suitable for signals with Nyquist sampling, when the input signal has a rectangular spectrum, and it is important to take into account the intrinsic frequency diversity effects associated to signals with larger than minimum Nyquist band. To overcome this problem, [15] employs an IMP (Inter-Modulation Product) approach to obtain the characterization of the signal being quantized at the corresponding BS. The quantization characteristic is strongly nonlinear, presenting a problem for the IMP approach, since the precision of the PSD of the quantized signal depends on the number of IMPs. Moreover, the quantization characteristic has multiple discontinuities and if the number of IMPs is too high this method increases the numerical computation, making this approach more adequate for smooth nonlinearities. To take advantage of the similarity of Gaussian-like characteristics of the received signals at each BS, [16] proposes an approach to obtain a small degree polynomial equivalent nonlinearity that provides signals with approximately the same spectral attributes as the quantized ones. Furthermore, the quantization noise variance that is obtained from the equivalent nonlinearity is very accurate even for oversampled signals. This paper presents robust receivers for evaluating the quantization effects as well as the different approaches for obtaining the statistical characteristics of the quantization noise.

This paper is organized as follows: in Section II the adopted cellular architecture considered in this paper and the receiver design is described. Section III is concerned with the different approaches for obtaining the spectral characteristics of the quantization noise and Section IV presents a set of performance results. Section V concludes the paper.

Throughout the paper we will adopt the following notations: bold letters denote vectors and matrices; $\mathbf{x}^*$, $\mathbf{x}^T$ and $\mathbf{x}^H$ denote complex conjugate, transpose and Hermitian (complex conjugate transpose) of $\mathbf{x}$, respectively. $\mathbf{I}_N$ denotes a $N \times N$ identity matrix and $\mathbf{e}_p$ is an appropriate column vector with 0 in all positions except the pth position that is 1. The expectation of x is denoted by $\mathbb{E}[x]$.

II. System Characterization

Fig. 1 illustrates the adopted cellular architecture considered in this paper. The system corresponds to a BS cooperation scheme characterized by fractionally overlapping cells, where each cell is associated to a specific BS. In this system, P MTs use the same frequency band to transmit the corresponding information (i. e., all MTs share the same physical channel), and there are R BSs that receive the MTs signals and can efficiently cooperate to improve the system's performance. In conventional systems each BS uniquely performs the detection of the signals of its own MTs and considers as interference the remaining information transmitted from the other MTs, thus discarding it. In turn, with BS cooperation systems the overall signals received at each BS are sent to a CPU that implements the separation of the different signals and then addresses them to the corresponding BS. Hence, the interference issues are managed and mitigated in the CPU. In order to decrease the amount of information to be transmitted in the backhaul link, the signals received at each BS are firstly quantized with an ADC block. In this paper, we assume perfect channel estimation [17] and synchronization, trough the assist of suitable training pilots and/or blocks [18], [19].

With respect to transmission, each MT employs an N size block with a SC-FDE modulation scheme. The data block $\{s_{n,p}; n = 0, 1, ..., N-1\}$ is associated with the pth MT ($p = 1, 2, ..., P$), where $s_{n,p}$ corresponds to a QPSK constellation symbol selected from the data following a given mapping scheme (e. g., a Gray mapping rule). Furthermore, the frequency-domain block is $\{S_{k,p}; k = 0, 1, ..., N-1\}$ = DFT $\{s_{n,p}\}$. In block transmission techniques an adequate cyclic prefix is appended to each data block and it is required to be longer than the overall impulse response, including channel effects as well as transmit and receive filters. However, in BS cooperation schemes it might be necessary to have a slightly longer cyclic prefix to account for different propagation periods between MTs and BSs, since the useful part of each block should overlap. After removing the samples associated with the cyclic prefix, at a given BS r ($r = 1, 2, ..., R$), the useful time-domain received block is given by

$$y_n^{(r)} = \sum_{p=1}^{P} \xi_{p,r} s_{n,p} \circledast h_{n,p}^{(r)} + \nu_n^{(r)}, \tag{1}$$

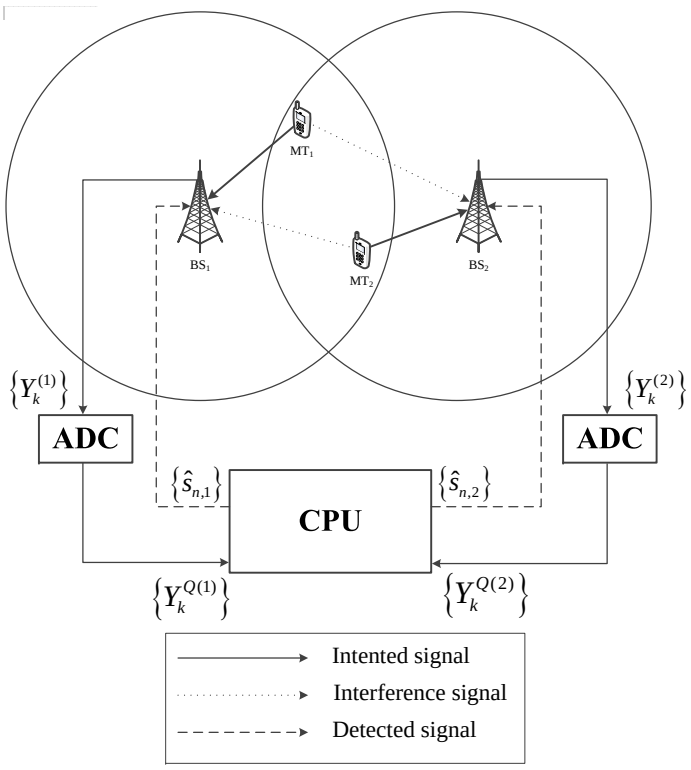

Fig. 1. Cellular scenario.

with $\circledast$ denoting the cyclic convolution regarding n. $h_{n,p}^{(r)}$ indicates the CIR (Channel Impulse Response) connecting the rth BS and the MT p, for for the nth time-domain element. The channel noise is denoted by $\nu_n^{(r)}$ and $\xi_{p,r}$ corresponds to a weighting parameter that accounts for the combined effects of power control and propagation loss effects, with the average received power associated with the pth MT at the rth BS corresponding to $|\xi_{p,r}|^2$. In the frequency-domain, $y_n^{(r)}$ is expressed by

$$Y_k^{(r)} = \sum_{p=1}^{P} \xi_{p,r} S_{k,p} H_{k,p}^{(r)} + N_k^{(r)}, \tag{2}$$

where $Y_k^{(r)}$ is the DFT of $y_n^{(r)}$. $H_{k,p}^{(r)}$ and $N_k^{(r)}$ are the frequency-domain components of $h_{n,p}^{(r)}$ and $\nu_n^{(r)}$, respectively, considering a normalized channel with $\sum_{n=1}^{N} \mathbb{E}\left[\left|h_{n,p}^{(r)}\right|^2\right] = 1$.

To decrease the amount of information to be transmitted through the backhaul link, at a given BS r the received time-domain signals $y_n^{(r)}$ are quantized, leading to $y_n^{Q(r)}$ and are expressed by

$$y_n^{Q(r)} = f_Q\left(\frac{\text{Re}\{y_n^{(r)}\}}{\sigma_y^{(r)}}\right)\sigma_y^{(r)} + j f_Q\left(\frac{\text{Im}\{y_n^{(r)}\}}{\sigma_y^{(r)}}\right)\sigma_y^{(r)}, \tag{3}$$

where $f_Q(\cdot)$ denotes the quantization characteristics and $\sigma_y^{(r)}$ the variance of the signal component. Since we are considering severely time-dispersive channels, with rich multipath propagation environment (the typical channel conditions behind SC-FDE schemes), the received time-domain samples $y_n^{(r)}$ can be accounted for as samples of a zero-mean complex Gaussian process, i.e., $y_n^{(r)} \sim \mathcal{CN}\left(0, 2{\sigma_y^{(r)}}^2\right)$, with

$$2{\sigma_y^{(r)}}^2 = \mathbb{E}\left[\left|y_n^{(r)}\right|^2\right] = \sum_{p=1}^{P} |\xi_{p,r}|^2 \mathbb{E}\left[|s_{n,p}|^2\right] + \mathbb{E}\left[\left|\nu_n^{(r)}\right|^2\right] = \sum_{p=1}^{P} |\xi_{p,r}|^2 2\sigma_s^2 + 2\sigma_\nu^2, \tag{4}$$

where

$$\sigma_s^2 = \mathbb{E}\left[|\text{Re}\{s_n\}|^2\right] = \mathbb{E}\left[|\text{Im}\{s_n\}|^2\right] \tag{5}$$

and

$$\sigma_\nu^2 = \mathbb{E}\left[|\text{Re}\{\nu_n\}|^2\right] = \mathbb{E}\left[|\text{Im}\{\nu_n\}|^2\right]. \tag{6}$$

Moreover, σ_s^2 and σ_ν^2 correspond to the symbol's and noise variance, respectively. According to the Bussgang's theorem [13], [20], the Gaussian nature of $y_n^{(r)}$ allows the quantized signals to be decomposed as the sum of uncorrelated useful and distortion terms, which leads to

$$y_n^{Q(r)} \approx \alpha y_n^{(r)} + d_n^{(r)}, \tag{7}$$

with $d_n^{(r)}$ denoting the quantization noise term. The α parameter is a constant which depends only on the nonlinear characteristic due to the quantization process, and can be computed as

$$\alpha = \int_{-\infty}^{\infty} \omega f_Q(\omega) \frac{1}{\sqrt{2\pi}} e^{-\frac{\omega^2}{2}} d\omega. \tag{8}$$

In the frequency-domain, the block associated with the quantized signal at the BS r corresponds to

$$Y_k^{Q(r)} \approx \alpha Y_k^{(r)} + D_k^{Q(r)} \approx \alpha \sum_{p=1}^{P} \xi_{p,r} S_{k,p} H_{k,p}^{(r)} + N_k^{Tot(r)}, \tag{9}$$

which is the DFE of the time-domain signal $y_n^{Q(r)}$. $N_k^{Tot(r)} = \alpha N_k^{(r)} + D_k^{(r)}$ accounts for the global noise from the transmitted and quantized signals.

When the transmissions from all P MTs to the R BSs in the system are taken into account, (9) can be expressed in a matrix format, given by

$$\mathbf{Y}_k^Q = \mathbf{H}_k^T \mathbf{S}_k + \alpha \mathbf{N}_k + \mathbf{D}_k, \tag{10}$$

with $\mathbf{Y}_k^Q = \left[Y_k^{Q(1)}, \ \ldots, Y_k^{Q(R)}\right]^T$, $\mathbf{S}_k = [S_{k,1}, \ \ldots, S_{k,P}]^T$, $\mathbf{N}_k = \left[N_k^{(1)}, \ \ldots, N_k^{(R)}\right]^T$, $\mathbf{D}_k = \left[D_k^{(1)}, \ \ldots, D_k^{(R)}\right]^T$,

$$\mathbf{H}_k^T = \begin{bmatrix} H_{k,1}^{eq^{(1)}} & \cdots & H_{k,P}^{eq^{(1)}} \\ \vdots & \ddots & \vdots \\ H_{k,1}^{eq^{(R)}} & \cdots & H_{k,P}^{eq^{(R)}} \end{bmatrix}, \tag{11}$$

and $H_{k,p}^{eq^{(r)}} = \alpha \xi_{p,r} H_{k,p}^{(r)}$.

The detection process relies on an iterative scheme based on the IB-DFE concept [7]. Here, the MTs are detected in a successive way taking advantage of the most updated estimates of the transmitted data symbols associated with each user to cancel the corresponding residual interference. Hence, this method can be regarded as a SIC (Successive Interference Cancelation) scheme, where the previous estimates are used to improve the detector accuracy. Moreover, at a given detection instance, the receiver takes into account the reliability of the symbol's estimates and implements interference cancelation to properly detect each MT.

Fixing a given iteration i, the estimated symbols associated with the pth MT $\{\hat{s}_{n,p}\}$ are the hard decisions of the time-domain detector output $\{\tilde{s}_{n,p}\}$ = IDFT $\{\tilde{S}_{k,p}\}$, where $\tilde{S}_{k,p}$ is given by

$$\tilde{S}_{k,p} = \mathbf{F}_{k,p}^T \mathbf{Y}_k^Q - \mathbf{B}_{k,p}^T \bar{\mathbf{S}}_{k,p}, \tag{12}$$

with $\mathbf{F}_{k,p}^T = \left[F_{k,p}^{(1)}, \ \ldots, F_{k,p}^{(R)}\right]^T$ and $\mathbf{B}_{k,p}^T = \left[B_{k,p}^{(1)}, \ \ldots, B_{k,p}^{(P)}\right]^T$ denoting the feedforward and feedback coefficients, respectively. $\bar{\mathbf{S}}_{k,p}$ is given by $\bar{\mathbf{S}}_{k,p} = \left[\bar{S}_{k,1}, \ldots, \bar{S}_{k,p-1}, \bar{S}_{k,p}, \ldots, \bar{S}_{k,P}\right]^T$, where block $\{\bar{S}_{k,p}\}$ is the DFT of the block of time-domain average values conditioned to the detector output $\{\bar{s}_{n,p}\}$. If $(p' < p)$ is considered, the elements of $\bar{\mathbf{S}}_{k,p'}$ are associated with the current iteration for the MTs already detected and with the previous iterations for the user that is being detected, and also with the MTs not yet detected in the current iteration.

For normalized QPSK constellations, i.e., $s_{n,p} = \pm 1 \pm j$, the average values $\bar{s}_{n,p}$ are given by [21], in which the BER (Bit Error Rate) is given by

$$P_e \simeq Q\left(\sqrt{\frac{1}{\theta_p}}\right), \tag{13}$$

where $Q(x)$ denotes the well known Gaussian error function and

$$\theta_p = \frac{1}{N^2} \sum_{k=0}^{N-1} \Theta_{k,p}, \tag{14}$$

with

$$\Theta_{k,p} = \mathbb{E}\left[\left|\tilde{S}_{k,p} - S_{k,p}\right|^2\right] = \mathbb{E}\left[\left|\mathbf{F}_{k,p}^T \mathbf{Y}_k^Q - \mathbf{B}_{k,p}^T \bar{\mathbf{S}}_{k,p} - S_{k,p}\right|^2\right]. \tag{15}$$

$\Theta_{k,p}$ designates the MSE (Mean Squared Error) of the frequency-domain samples $\tilde{S}_{k,p}$ [21]. The processing of $\Theta_{k,p}$ is concerned with the evaluation of the optimum values of coefficients $\mathbf{F}$ and $\mathbf{B}$, which requires the minimization of $\Theta_{k,p}$. For simplicity purposes we drop the dependence of k in the matrices definitions. The optimum feedforward coefficient $\mathbf{F}$ is obtained by defining

$$\mathbf{F}' = \mathbf{\Lambda}\mathbf{H}^H \mathbf{e}_p, \tag{16}$$

with

$$\mathbf{\Lambda} = \left(\mathbf{H}^H \left(\mathbf{I}_P - \mathbf{P}^2\right) \mathbf{H} + \mathbf{R}_{N^{Tot}} \mathbf{R}_S^{-1} \left|\alpha\right|^{-2}\right)^{-1}, \tag{17}$$

with $\mathbf{R}_S = \mathbb{E}\left[\mathbf{S}^* \mathbf{S}^T\right] = 2\sigma_S^2 \mathbf{I}_P$ and $\mathbf{R}_{N^{Tot}} = \mathbb{E}\left[\mathbf{N^{Tot}}^* \mathbf{N^{Tot}}^T\right] = \left|\alpha\right|^2 \mathbf{R}_N + \mathbf{R}_D$, being the correlation matrices of $\mathbf{S}$ and $\mathbf{N^{Tot}}$ respectively. $\mathbf{R}_N = 2\sigma_N^2 \mathbf{I}_R$ and $\mathbf{R}_D = 2\text{diag}(\sigma_D^{(1)^2}, \sigma_D^{(2)^2}, ..., \sigma_D^{(R)^2})$ are the correlations matrices for the channel noise and quantization noise, respectively, and σ_S^2 and σ_N^2 denote the symbol's and noise's variance, in the frequency-domain, respectively. We can define an average overall channel frequency response γ_p as

$$\gamma_p = \frac{1}{N} \sum_{k=0}^{N-1} \sum_{r=1}^{R} F_{k,p}^{(r)} H_{k,p}^{eq(r)} = 1, \tag{18}$$

in order to have a normalized FDE with $\mathbb{E}\left[\tilde{s}_{n,p}\right] = s_{n,p}$. Therefore, taking into account (16) we can say that

$$\mathbf{F} = \kappa \mathbf{F}', \tag{19}$$

in which κ to a normalization factor related to γ_p as

$$\kappa = \frac{1}{\gamma_p}. \tag{20}$$

The feedback coefficient $\mathbf{B}$ is expressed by

$$\mathbf{B} = \alpha \mathbf{H}\mathbf{F} - \mathbf{e}_p. \tag{21}$$

Furthermore, according to [21] a measure for the reliability of the estimates within the ith iteration can be defined, designated as correlation coefficients, and is given by

$$\rho_p = \frac{\mathbb{E}\left[\hat{s}_{n,p} s_{n,p}^*\right]}{\mathbb{E}\left[\left|s_{n,p}\right|^2\right]}. \tag{22}$$

Clearly, the robust receiver described above requires the knowledge of the variance of the quantization noise σ_d^2, which in the general case is a function of k (i.e., it is not flat in the frequency). This means that we need to obtain its spectral characterization, which in general is not simple. In the next section we present analytical tools for obtaining this spectral characterization.

III. Spectral characterization of the quantization noise

This section presents the different approaches to obtain the spectral characterization of the quantization noise. Consequently, we are interested in the derivation of the quantization noise variance $\sigma_D^2(k)$, for each frequency component. Following equation (3), $f_Q(\cdot)$ represents a "mid-rise" quantizer with a normalized saturation level of $\frac{A_M}{\sigma_y^{(r)}}$ and m bits of resolution for the real and imaginary parts of a given quantized sample. The quantization step is denoted by Δ and is given by $\Delta = \frac{2A_M}{2^m - 1}$.

To obtain the spectral characteristics of the quantization noise, the basic approach is to consider that the quantization noise has a constant PSD (i.e., a flat spectrum) and its power is given by $\frac{\Delta^2}{12}$ [12]. This approach is only appropriated when the

input signals have a rectangular form, not oversampled, and the quantizers are linear with inconsequential saturation effects, meaning $A_M/\sigma = +\infty$.

Another approach is to consider that in the quantization process the input signals have Gaussian characteristics, with the output signals expressed as in (7). At the rth BS, when the signal to be quantized has a flat spectrum, the quantization noise frequency characteristics are also flat and according to [13] its variance can be expressed as

$$\sigma_d^{(r)^2} = \sigma_{y^Q}^{(r)^2} - |\alpha|^2 \, 2\sigma_y^{(r)^2}, \tag{23}$$

with $\sigma_y^{(r)^2}$ designating the average power of the input signal and the output power $\sigma_{y^Q}^{(r)^2}$ given by

$$\sigma_{y^Q}^{(r)^2} = 2\int_{-\infty}^{+\infty} f^2(y)p(y)dy. \tag{24}$$

Despite this approach accounting for quantization noise and saturation effects, it is only suitable for signals with Nyquist sampling and when the input signal has a rectangular spectrum.

The method presented in [15] theoretically characterizes the quantization noise through an IMP (Inter-Modulation Product) measurement, which is suitable for signal inputs that have arbitrary spectral distributions (i.e., they are not rectangular) and/or for oversampled signals. With this approach, the idea is to obtain the spectral distributions of the distinct inter-modulation products at the quantizer output and add them to obtain the PSD of the quantized signal. The accuracy of the PSD of the quantized signal depends on the number of IMPs, since the larger the number of IMPs, the better the accuracy. As a consequence, despite this approach works well for smooth nonlinearities, it may present complexity and/or convergence problems when the nonlinearities are severe. Some quantizers present low number of bits of resolution and/or low clipping levels, which fall into the cases where nonlinearities are severe, requiring an approximation by a large number of polynomial terms. According to [15], the PSD of the quantized signal is obtained through the DFT of the output autocorrelation

$$G_{y^Q,k} = \text{DFT}\left(R_{y^Q,n}\right), \tag{25}$$

where $R_{y^Q,n}$ is expressed by

$$R_{y^Q,n} = \sum_{\gamma=0}^{+\infty} 2P_{2\gamma+1} \frac{\left(R_{y,n}\right)^{2\gamma+1} + j\left(\text{Im}R_{y,n}\right)^{2\gamma+1}}{R_{y,0}^{2\gamma+1}}, \tag{26}$$

in which $R_{y,0} = 2\sigma_y^2$ indicates the input signal average power. $P_{2\gamma+1}$ designates the power associated with the inter-modulation product of order $2\gamma+1$ and is defined as

$$P_{2\gamma+1} = \frac{\left(\int_{-\infty}^{+\infty} f(y)p(y)H_{2\gamma+1}\left(\frac{y}{\sqrt{2}\sigma_y}\right)dy\right)^2}{2^{2\gamma+a}\,(2\gamma+1)!}, \tag{27}$$

with $H_{2\gamma+1(\cdot)}$ indicating the Hermite polynomial of order $2\gamma+1$ and $f(y)$ the quantizer characteristics. This approach is difficult since it requires a high number of IMPs n_γ when (26) is being truncated for the polynomial approximation. Fig. 2 illustrates the simulated and the theoretical PSD of a quantized signal for $n_\gamma = 2$ and $n_\gamma = 10$. The quantizer is characterized by employing $m = 2$ resolution bits and has a normalized saturation level of $A_M/\sigma = 0.5$. For the transmission, $P = 2$ MTs are considered and the blocks have a size of $N = 512$ symbols. Moreover, an oversampling factor of $M = 2$ and time-dispersive channels with 32 rays in the multipath environment are taken into account. Fig. 2 shows that when $n_\gamma = 2$ there are considerable differences between the simulated and theoretical results in both the in-band and out-of-band regions. It can be seen that the results are only approximately matched in the in-band part of the spectrum and when $n_\gamma = 10$. The out-of-band region demonstrates the convergence and/or complexity issues in this approach, since there is a significant difference between simulated and theoretical results. Fig. 3 shows the spectrum of a quantized signal received at a given BS. The number of MTs transmitting is $P = 3$, the transmission block size is $N = 512$ with $M = 2$ oversampling factor and there are 32 rays in the multipath profile between each MT and the BS. That illustrates the total PSD of the quantized signal obtained with expression (26) and the spectral distributions of the IMP of order $2\gamma+1$. It is possible to notice that the PSD of P_5, which is associated to the IMP of $\gamma = 2$ has very low fluctuations and it is almost constant regarding the $P_7\,(\gamma = 3)$ case. In the time-domain, the autocorrelations of these PSDs can be approximated by Dirac delta functions. This means that all autocorrelations from a given order $\gamma = \gamma_{max}$ can be approximated in the autocorrelation associated to the IMP of order $\gamma = \gamma_{max}$, that concentrates the power of the IMPs from $\gamma = \gamma_{max}$ to $\gamma = +\infty$. Following this idea, and taking into account the issues presented with the previous approach, [16] proposes a method to obtain an equivalent nonlinearity $g(y)$, in which the IMPs are related to the

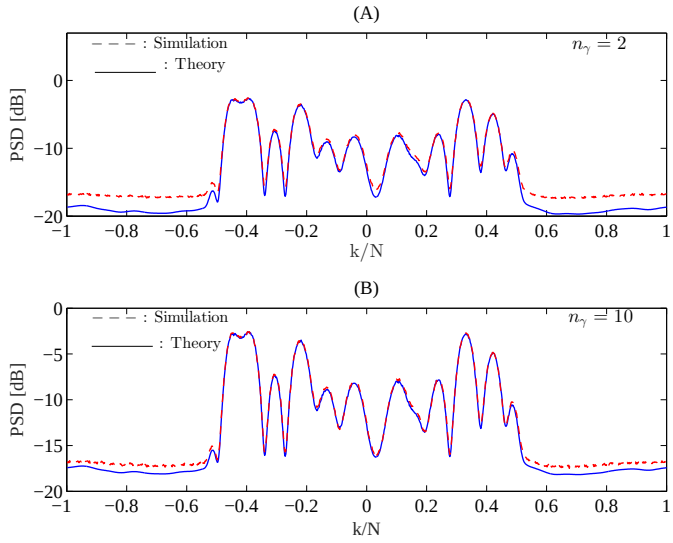

Fig. 2. PSD of a quantized signal obtained with $n_\gamma = 2$ (A) and with $n_\gamma = 10$ (B).

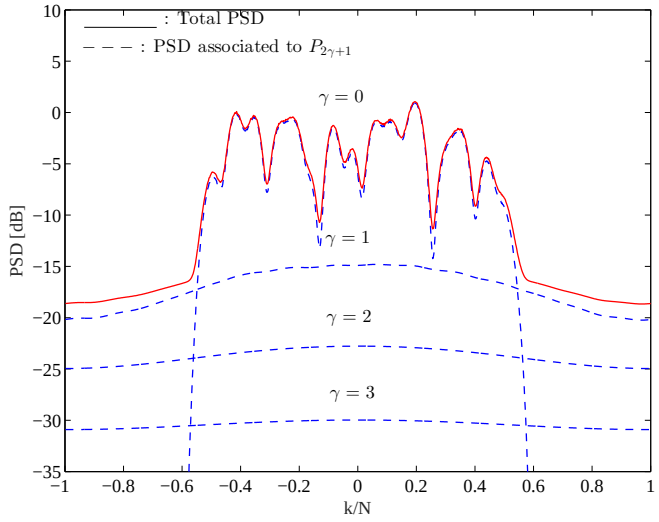

Fig. 3. PSD of a quantized signal and the individual spectral distributions of the IMPs of order $2\gamma + 1$.

IMPs of $f(y)$ according to

$$P^g_{2\gamma+1} = \begin{cases} P^f_{2\gamma+1}, & 0 \le \gamma < \gamma_{\max} \\ P^f_{\text{out}} - \sum_{\gamma=0}^{\gamma_{\max}-1} P^f_{2\gamma+1}, & \gamma = \gamma_{\max} \\ 0, & \gamma \ge \gamma_{\max}, \end{cases} \tag{28}$$

with P^f_{out} given by (24) and the value of γ_{max} being selected to ensure that the PSD of the IMP of order $2\gamma_{max}+1$ is constant. The use of the superscript f or g differentiates between the conventional quantization characteristics and the equivalent nonlinearity, respectively.

So, the equivalent nonlinearity, designated as $g(x)$ is expressed by

$$g(y) = \sum_{\gamma'=0}^{\gamma_{max}} T_{\gamma'} y^{2\gamma'+1}, \tag{29}$$

in which $\{T_{\gamma'}; \gamma' = 0, 1, ..., \gamma_{max}\}$ indicate the polynomial coefficients. To obtain these coefficients it is necessary to relate the IMPs power of $g(y)$ with the corresponding expression. Since there is not a linear relation with them, as the definition of

the power associated to a given IMP shows (see (27)), the IMPs of $g(y)$ are redefined by

$$P^{g}_{2\gamma+1} = \frac{\left(\nu^{g}_{2\gamma+1}\right)^2}{2^{2\gamma+1}(2\gamma+1)!}, \tag{30}$$

where the coefficients $\{\nu^{g}_{2\gamma+1}; \gamma = 0, 1, ..., \gamma_{\max}\}$ are expressed as

$$\begin{aligned}\nu^{g}_{2\gamma+1} &= \int_{-\infty}^{+\infty} g(y)p(y)H_{2\gamma+1}\left(\frac{y}{\sqrt{2}\sigma_y}\right)\mathrm{d}y \\ &= \sqrt{P^{g}_{2\gamma+1}}\sqrt{2^{2\gamma+1}(2\gamma+1)!}.\end{aligned} \tag{31}$$

Clearly, in (31), the coefficients $\{\nu^{g}_{2\gamma+1}; \gamma = 0, 1, ..., \gamma_{max}\}$ have a linear relation with $g(y)$. Furthermore, the polynomial coefficients $\{T_{\gamma'}; \gamma' = 0, 1, ..., \gamma_{max}\}$ can be obtained by substituting (29) in the first line of (31), expressed as

$$\begin{aligned}\nu^{g}_{2\gamma+1} &= \int_{-\infty}^{+\infty}\sum_{\gamma'=0}^{\gamma_{\max}} T_{\gamma'}y^{2\gamma'+1}p(y)H_{2\gamma+1}\left(\frac{y}{\sqrt{2}\sigma_y}\right)\mathrm{d}y \\ &= \sum_{\gamma'=0}^{\gamma_{\max}} T_{\gamma'}\underbrace{\int_{-\infty}^{+\infty} y^{2\gamma'+1}p(y)H_{2\gamma+1}\left(\frac{y}{\sqrt{2}\sigma_y}\right)\mathrm{d}y}_{\beta_{\gamma\gamma'}} \\ &= \sum_{\gamma'=0}^{\gamma_{\max}} \beta_{\gamma\gamma'}T_{\gamma'}.\end{aligned} \tag{32}$$

In Fig. 4 one can notice that the equivalent nonlinearity $g(y)$ approach presents a smoother quantization characteristic when compared to the conventional one, represented by $f(y)$. The quantizer is characterized by a saturation level of $A_M/\sigma_y = 1$ and $m = 3$ bits of resolution. With this approach, the spectral characterization of the quantization noise $\sigma^2_D(k)$ can be shown in Fig.

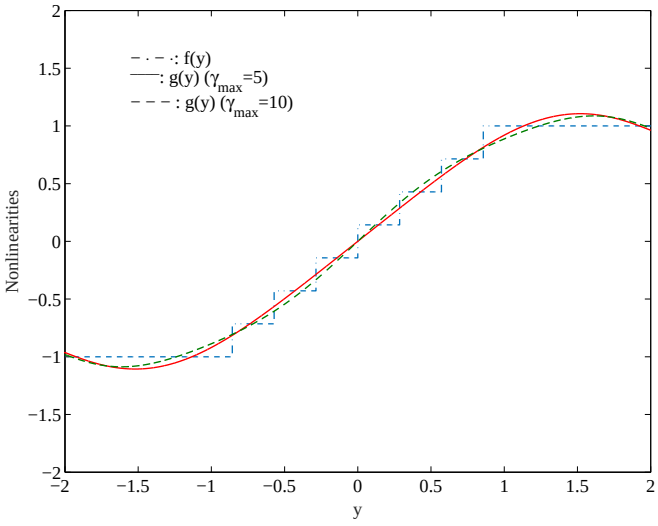

Fig. 4. Quantizer characteristic and its equivalent nonlinearity considering $\gamma_{max} = 5$ and $\gamma_{max} = 10$.

5, which illustrates the theoretical and simulation results. The signal received at a given BS is a sum of all the contributions from $P = 3$ MTs with a single transmission block having size of $N = 512$. We consider 32 rays in the multipath propagation environment and the oversampling factor is $M = 2$. Furthermore, the quantizer is characterized by the employment of $m = 4$ resolution bits and a normalized clipping level of $A_M/\sigma_y = 1$. From Fig. 5 it can be seen that the average PSD approach is not adequate when one takes into account the oversampling effects. The PSD obtained through the equivalent nonlinearity approach is very accurate even for a reduced amount of terms (i.e., $\gamma_{max} = 5$), contrarily to the IMP analysis approach, which

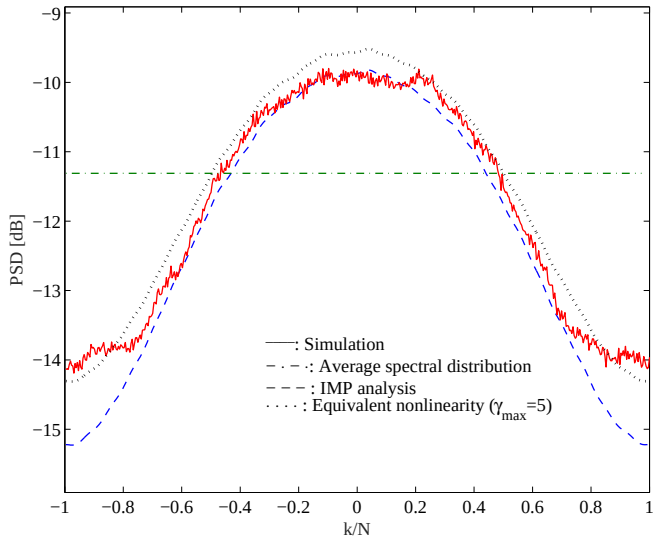

Fig. 5. Spectral characterization of the quantization noise obtained theoretically and by simulation. Comparison of several approaches considering an oversampling factor of $M = 2$.

presents a higher complexity methodology. Hence, the IMP analysis method requires $n_\gamma = 10$ to provide the same accuracy when the equivalent nonlinearity approach is considered. Furthermore, even for a large number of IMPs, the IMP analysis approach presents considerable errors in the out-of-band region when compared to the results obtained by simulation.

Considering the spectral characteristics of the quantization noise, it is possible to analyze in Fig. 6 the evolution of the average value of the PSD as in function of the normalized clipping level A_M/σ_y obtained by theory and simulation. The

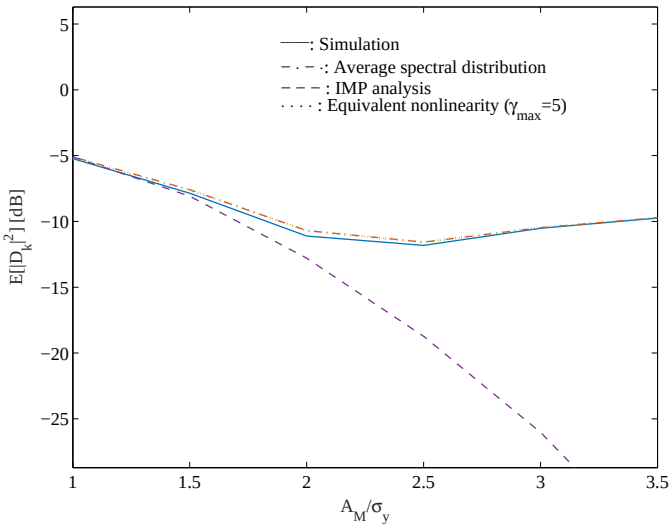

Fig. 6. Average PSD of the quantization noise obtained theoretically and by simulation. Comparison of several approaches without oversampling ($M = 1$).

signal received at the BS and the quantizer characteristics are the same as in Fig. 5, however there is no oversampling considered (i.e., $M = 1$). Clearly, the IMP analysis approach has less accuracy for high values of the normalized saturation level, even for a high number of IMPs $n_\gamma = 10$. On the other hand, the equivalent nonlinearity approach with $\gamma_{max} = 5$ is very accurate, and its results are very close to the ones obtained by simulation.

IV. Performance Results

Section III presented several methodologies to obtain the spectral characterization of the quantization noise and in this section we discuss a set of performance results in order to evaluate those approaches. The different methods for obtaining

the quantization noise characteristics are applied to the discussed iterative frequency-domain receivers for the uplink of BS cooperation schemes employing SC-FDE modulations. The blocks associated with the transmission of each MT have N data symbols, selected from a QPSK constellation under a Gray mapping rule. Furthermore, an oversampling factor of M was considered. The transmission channels between the MTs and the BSs are severely time-dispersive with I symbols-spaced taps and uncorrelated Rayleigh fading on the different multipath components. Moreover, it is assumed that the channels are uncorrelated and that there is a perfect synchronization and channel estimation. The quantization process is defined by a "mid-rise" quantizer employing m resolution bits and a normalized saturation level A_M/σ. When the performance results are presented following a BER (Bit Error Rate) measure, the MFB (Matched Filter Bound) is included for the sake of comparison.

Analyzing the influence of the oversampling factor, Fig. 7 illustrates the distortion caused by the quantization process (i.e., spectrum of the quantization noise) when the received signal is the sum of the signals transmitted from $P = 2$ MTs. Each block has size of $N = 256$ and $I = 64$ multipath rays were considered. The quantizer is characterized by the employment

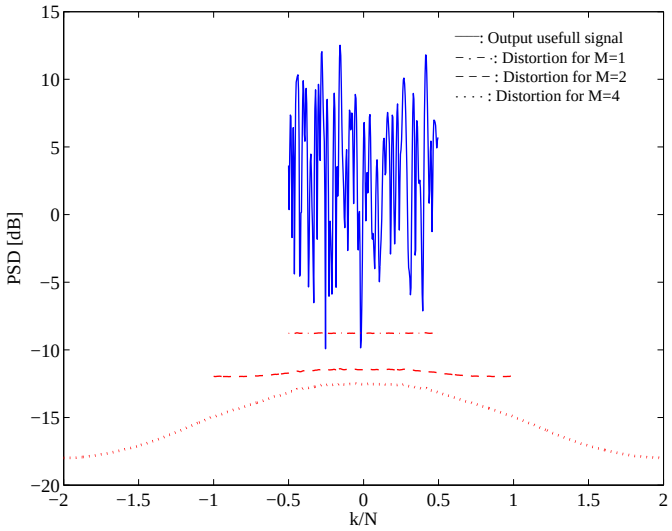

Fig. 7. Quantization noise spectrum for different oversampling factors.

of $m = 3$ resolution bits and there are three values of the oversampling factor are taken into account, $M = 1$ (where there is no oversampling), $M = 2$ and $M = 4$. Clearly, there is a higher value for the degradation when the oversampling factor approaches 1 due to aliasing issues. Moreover, since the spectrum from distortion is almost constant and the one from the output signal has a lot of fluctuations, the SIR (Signal-to-Interference Ratio) can be very low for frequencies in deep fade. One can notice that when M changes from 1 to 2 there is a gain of approximately 2 dB. Moreover, when the resolution bits are $2m$ instead of m it is possible to have gains of $6m$ dB, which indicates that the best option is to increase the resolution bits instead of the oversampling factor M. For this reason, the following performance results do not consider signals with oversampling (i.e., $M > 1$).

Fig. 8 illustrates the BER performance of a BS cooperation scenario with $P = 2$ MTs and $R = 2$ BSs. In this case we do not consider any quantization performed on the transmitted data. The power associated with the different transmission links is $\xi_{p,r} = 0$ dB, where all MTs transmit with the same average power to all BSs. For simplicity purposes the 3rd iteration is omitted, since it does not add any relevant information. As shown, there is a performance improvement from the 1st iteration till the 4th. This improvement is higher for the linear FDE (1st iteration), which is due to the higher residual ISI at the FDE output, and the performance of the iterative receiver is already close to the MFB after just 4 iterations. Moreover, the 1st MT has a worst performance when comparing to the 2nd MT. This is due to the fact that when the 2nd MT is detected the detector already has information relating to the separation for the 1st MT. Clearly, the information provided from the detection of the 1st MT contributes to an accurate detection for the 2nd MT.

Regarding the scenario illustrated in Fig. 8, Fig. 9 and Fig. 10 show, for the 1st and 2nd MTs, respectively, the comparison of results when quantization is employed. The quantizer is characterized by the use of $m = 3$ and $m = 4$ resolution bits and it is considered a conventional approach for the receiver (designated as "Conv. Rx"), in which the quantization effects are not taken into account. This means that the distortion from the quantization noise is $\sigma_d^2 = 0$. As expected, when quantization is employed there is a degradation on the performance, specially for lower values of m and higher values of SNR.

Fig. 11 and Fig. 12 illustrate the BER performance for a scenario with quantization when "Conv. Rx" and "Robust Rx" are considered. With the "Robust Rx", the receiver takes into account the spectral characterization of the quantization noise

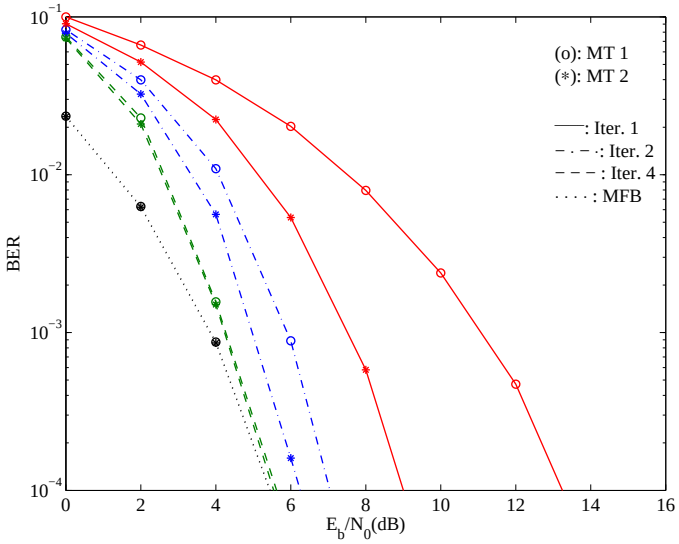

Fig. 8. BER performance for a BS cooperation scenario with $P = 2$ MTs, $R = 2$ BSs and without quantization.

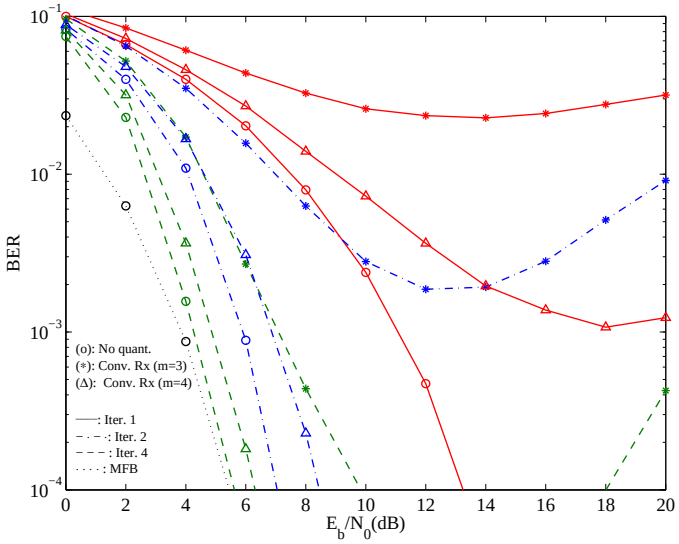

Fig. 9. BER performance for a BS cooperation scenario with $P = 2$ MTs and $R = 2$ BSs. Comparison of results without quantization and quantization with $m = 3$ and 4 bits of resolution employing a conventional receiver (1st MT).

following the method described with the equivalent nonlinearities approach. Furthermore, for the detection with this method the γ_{max} parameter corresponds to $\gamma_{max} = 6$. Both figures demonstrate worst performance results when the "Conv. Rx" is considered, especially for high values of SNR. Moreover, one can notice that the robust receivers (that account for $\sigma_D^2(k)$) can cope with the degradation provided by the employment of conventional receivers.

For the 1st and 2nd MTs, respectively, Fig. 13 and Fig. 14 compare the quantization effects of the "Robust Rx" results with a simplified version of the robust receiver, designated as "Simp. Robust Rx". In the "Simp. Robust Rx" receiver the quantization noise characteristics are given by equation (23), which can be seen as an average value of the spectral distribution for the quantization noise. From these figures it can be noticed that the results from the "Simp. Robust Rx" are similar to those provided by the full robust version, which indicates that the approach used in the "Robust Rx" does not present a clear advantage in terms of compensating of having a higher complex method for obtaining the spectral characterization of the quantization noise in the considered iterative receivers.

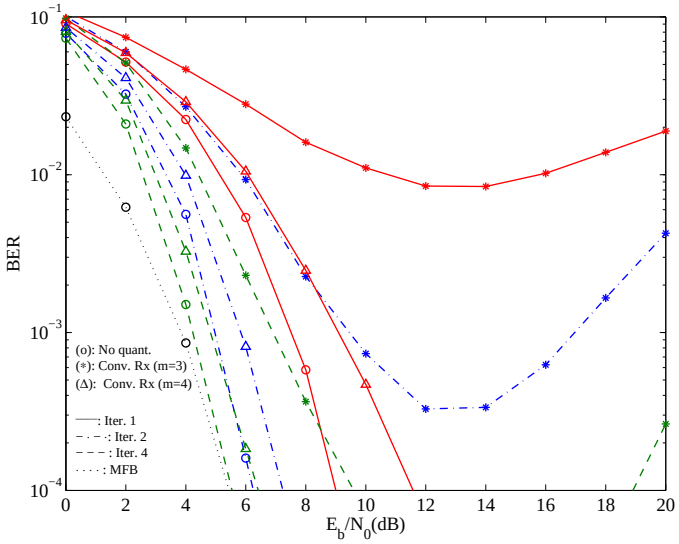

Fig. 10. BER performance for a BS cooperation scenario with $P = 2$ MTs and $R = 2$ BSs. Comparison of results without quantization and quantization with $m = 3$ and 4 bits of resolution employing a conventional receiver (2nd MT).

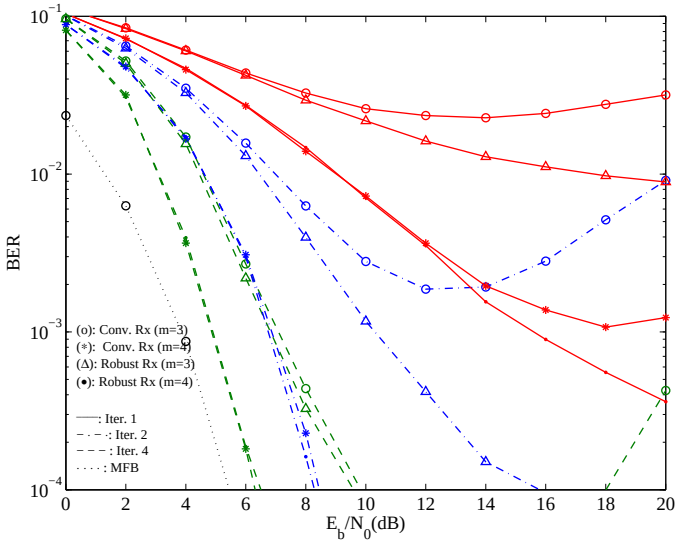

Fig. 11. BER performance for a BS cooperation scenario with $P = 2$ MTs and $R = 2$ BSs. Comparison of results with quantization with $m = 3$ and 4 bits of resolution employing a conventional and robust receivers (1st MT).

V. Conclusions

This paper analyzed the quantization effects in the uplink of BS cooperation systems with SC-FDE modulations and iterative receivers based on the IB-DFE concept. This work was centered on the performance of robust receivers that can account for different methods of obtaining the spectral characterization of the quantization noise. The results shown that the considered receivers allow significant performance improvements, especially when low-resolution quantizers are employed. Moreover, we presented a simplified version for the receiver that can substitute the approach of defining an equivalent nonlinearity that may substitute the conventional quantization characteristics. Our results showed a very good agreement for the performance values which are quite acceptable when the quantization employs $m = 4$ bits of resolution.

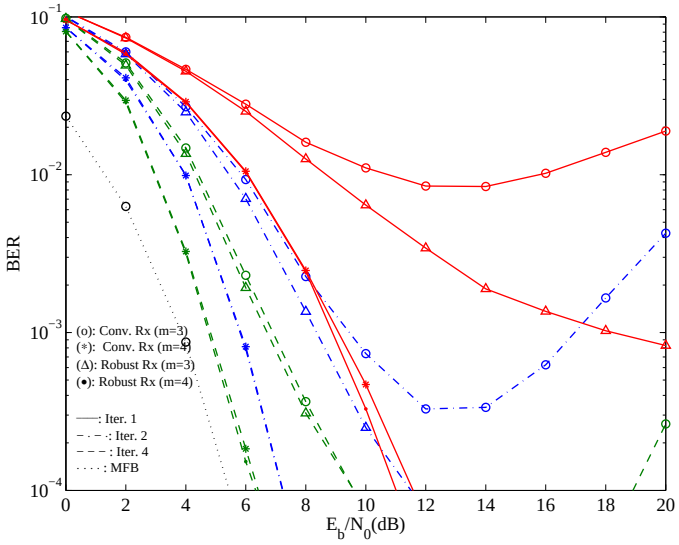

Fig. 12. BER performance for a BS cooperation scenario with $P = 2$ MTs and $R = 2$ BSs. Comparison of results with quantization with $m = 3$ and 4 bits of resolution employing a conventional and robust receivers (2nd MT).

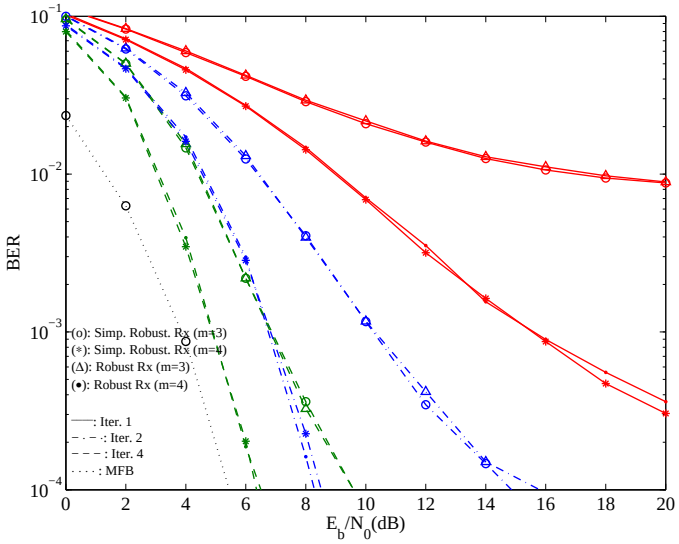

Fig. 13. BER performance for a BS cooperation scenario with $P = 2$ MTs and $R = 2$ BSs. Comparison of results with quantization with $m = 3$ and 4 bits of resolution employing simplified robust and robust receivers (1st MT).

ACKNOWLEDGMENT

This work was partially supported by Instituto de Telecomunicações and Fundação para a Ciência e a Tecnologia (FCT) under the project PURE-5GNET IT pluriannual founding and PhD grant SFRH/BD/87524/2012.

REFERENCES

[1] F. C. Ribeiro, J. Guerreiro, R. Dinis, F. Cercas, and A. Silva, "On the Design of Robust Multi-User Receivers for Base Station Cooperation Systems," in *Vehicular Technology Conference (VTC Fall), 2016 IEEE*, Sept 2016, pp. 1–7.

[2] O. Somekh, B. Zaidel, and S. Shamai, "Sum Rate Characterization of Joint Multiple Cell-Site Processing," *IEEE Transactions on, Information Theory*, vol. 53, no. 12, pp. 4473 –4497, Dec. 2007.

[3] E. Bjo Andrnson, R. Zakhour, D. Gesbert, and B. Ottersten, "Cooperative Multicell Precoding: Rate Region Characterization and Distributed Strategies With Instantaneous and Statistical CSI," *IEEE Transactions on, Signal Processing*, vol. 58, no. 8, pp. 4298–4310, aug. 2010.

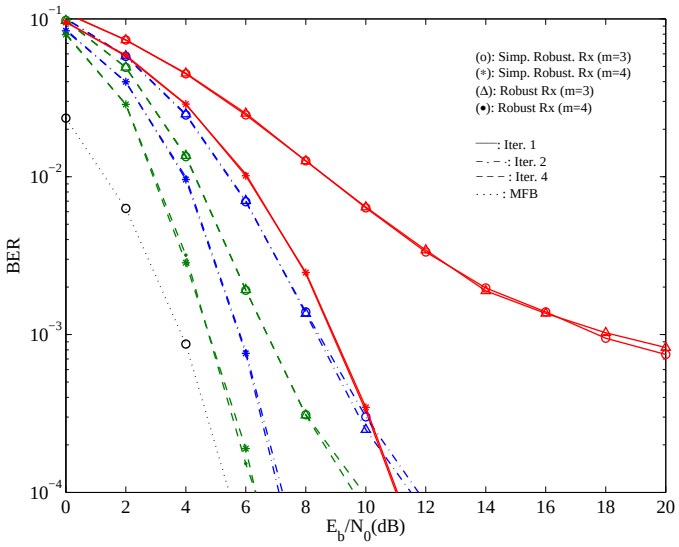

Fig. 14. BER performance for a BS cooperation scenario with $P = 2$ MTs and $R = 2$ BSs. Comparison of results with quantization with $m = 3$ and 4 bits of resolution employing simplified robust and robust receivers (2nd MT).

[4] D. Gesbert, S. Hanly, H. Huang, S. Shamai Shitz, O. Simeone, and W. Yu, "Multi-Cell MIMO Cooperative Networks: A New Look at Interference," *IEEE Journal on, Selected Areas in Communications*, vol. 28, no. 9, pp. 1380 –1408, Dec. 2010.

[5] L. Cimini, "Analysis and Simulation of a Digital Mobile Channel Using Orthogonal Frequency Division Multiplexing," *Communications, IEEE Transactions on*, vol. 33, no. 7, pp. 665–675, Jul 1985.

[6] H. Sari, G. Karam, and I. Jeanclaude, "An analysis of orthogonal frequency-division multiplexing for mobile radio applications," in *Vehicular Technology Conference, 1994 IEEE 44th*, Jun 1994, pp. 1635–1639 vol.3.

[7] N. Benvenuto, R. Dinis, D. Falconer, and S. Tomasin, "Single Carrier Modulation With Nonlinear Frequency Domain Equalization: An Idea Whose Time Has Come Again," *Proceedings of the IEEE*, vol. 98, no. 1, pp. 69 –96, Jan. 2010.

[8] A. Gusmão, R. Dinis, J. Conceicão, and N. Esteves, "Comparison of Two Modulation Choices for Broadband Wireless Communications," in *Vehicular Technology Conference Proceedings, 2000. VTC 2000-Spring Tokyo. 2000 IEEE 51st*, vol. 2, May 2000, pp. 1300 –1305 vol.2.

[9] D. Falconer, S. Ariyavisitakul, A. Benyamin-Seeyar, and B. Eidson, "Frequency Domain Equalization for Single-Carrier Broadband Wireless Systems," *IEEE, Communications Magazine*, vol. 40, no. 4, pp. 58–66, Apr. 2002.

[10] R. Dinis, R. Kalbasi, D. Falconer, and A. Banihashemi, "Iterative Layered Space-Time Receivers for Single-Carrier Transmission over Severe Time-Dispersive Channels," *IEEE, Communications Letters*, vol. 8, no. 9, pp. 579 – 581, Sep. 2004.

[11] R. Kalbasi, R. Dinis, D. Falconer, and A. Banihashemi, "An iterative frequency-domain layered space-time receiver for SDMA systems with single-carrier transmission," in *Acoustics, Speech, and Signal Processing, 2004. Proceedings. (ICASSP '04). IEEE International Conference on*, vol. 4, may 2004, pp. iv–793–iv–796 vol.4.

[12] J. Proakis and M. Salehi, *Digital Communications*, 5th ed. Mc-Graw Hill, 2007.

[13] H. E. Rowe, "Memoryless Nonlinearities With Gaussian Inputs: Elementary Results," *The Bell System Technical Journal*, vol. 61, no. 7, pp. 1519–1525, 1982.

[14] F. C. Ribeiro, R. Dinis, F. Cercas, and A. Silva, "Receiver Design for the Uplink of Base Station Cooperation Systems employing SC-FDE Modulations," *EURASIP Journal on Wireless Communications and Networking*, vol. 2015, no. 1, Jan. 2015.

[15] T. Araújo and R. Dinis, "Performance Evaluation of Quantization Effects on Multicarrier Modulated Signals," *IEEE Transactions on, Vehicular Technology*, vol. 56, no. 5, pp. 2922–2930, 2007.

[16] P. M. João Guerreiro, Rui Dinis, "Use of equivalent nonlinearities for studying quantisation effects on sampled multicarrier signals," *Electronics Letters*, vol. 51, pp. 151–153(2), January 2015.

[17] N. Souto, R. Dinis, and J. Silva, "Impact of Channel Estimation Errors on SC-FDE Systems," *Communications, IEEE Transactions on*, vol. 62, no. 5, pp. 1530–1540, May 2014.

[18] F. Coelho, R. Dinis, and P. Montezuma, "Joint Detection and Channel Estimation for Block Transmission Schemes," in *MILITARY COMMUNICATIONS CONFERENCE, 2010 - MILCOM 2010*, Oct 2010, pp. 1765–1770.

[19] ——, “Efficient Channel Estimation for Single Frequency Broadcast Systems,” in *Vehicular Technology Conference (VTC Fall), 2011 IEEE*, Sept 2011, pp. 1–6.

[20] J. J. Bussgang, “Crosscorrelation functions of amplitude-distorted gaussian signals,” 1952.

[21] P. Silva and R. Dinis, *Frequency-Domain Multiuser Detection for CDMA Systems*. River Publishers, 2012.